Chapter 6

Quasi-parallel Shock Structure and Processes

D. Burgess[1], E. A. Lucek[2], M. Scholer[3], S. D. Bale[4], M. A. Balikhin[5], A. Balogh[2], T. S. Horbury[2], V. V. Krasnoselskikh[6], H. Kucharek[7], B. Lembège[8], E. Möbius[7 9], S. J. Schwartz[1 10], M. F. Thomsen[11], and S. N. Walker[5]

6.1 Introduction

When the interplanetary magnetic field is oriented such that the angle between the upstream magnetic field and the nominal bow shock normal is small ($\theta_{Bn} < 45^\circ$), a much more complex shock is observed than in the quasi-perpendicular case. Historically, this has made interpreting single spacecraft data more difficult, so that for a long time the quasi-parallel shock remained relatively poorly understood. The difficulties arise, as we now understand, because the supercritical quasi-parallel shock is a spatially extended and inhomogeneous transition, with smaller length-scale features cyclically reforming within it.

[1]Astronomy Unit, Queen Mary, University of London, London, UK
[2]Space and Atmospheric Physics, The Blackett Laboratory, Imperial College London, London, UK
[3]Max-Planck-Institut für extraterrestrische Physik, Garching, Germany
[4]Department of Physics and Space Sciences Laboratory, University of California, Berkeley, CA, USA
[5]Automatic Control and Systems Engineering, University of Sheffield, Sheffield, UK
[6]LPCE/CNRS, Orléans, France
[7]Space Science Center, Institute for the Study of Earth, Oceans, and Space, University of New Hampshire, Durham, New Hampshire, USA
[8]CETP/IPSL, Velizy, France
[9]Also Department of Physics, University of New Hampshire, Durham, New Hampshire, USA
[10]Now at Space and Atmospheric Physics, The Blackett Laboratory, Imperial College London, London, UK
[11]Los Alamos National Laboratory, Los Alamos, NM, USA

Space Science Reviews 118: 205–222, 2005.
DOI: 10.1007/s11214-005-3832-3

Under the quasi-parallel magnetic geometry ions are able to escape into the region upstream of the shock (e.g., Gosling et al., 1982), where they give rise to and interact with the waves which populate the foreshock (e.g., Le and Russell, 1992), as discussed in Eastwood et al. (2005, this issue). Of particular importance is the association of energetic ions (10–300 keV) with the foreshock and quasi-parallel shock. The role of the quasi-parallel shock as the site of particle acceleration has been fundamental in the development and testing of theories of particle acceleration. The understanding gained has direct implications for other solar system and astrophysical shocks. Recent advances in this area are discussed in Section 6.3.

Before the launch of Cluster a picture of the quasi-parallel shock had been developed from single and dual spacecraft observations, together with results from numerical simulations. Observations of the magnetic field strength changes within the shock showed that they could not all be explained simply by the in-and-out motion of a single shock surface, which would produce nested signatures. A nested signature arises when the boundary crossings observed at one spacecraft are contained, in time, within those observed by a second spacecraft. Instead there were coherent, short scale, magnetic pulsations embedded within the overall transition. These pulsations had sunward directed velocities, but were convected anti-sunwards in the solar wind plasma flow (e.g., Thomsen et al., 1988).

A standard model was developed in which the quasi-parallel shock transition was viewed as being composed of a patchwork of magnetic field enhancements, which grew from the interaction between upstream waves propagating sunward in the plasma frame and a gradient in the supra-thermal particle pressure (e.g., Giacalone et al., 1993; Dubouloz and Scholer, 1995). These field enhancements were characterised by a region where the magnetic field magnitude was a factor of ≥ 4 or so greater than the background field. They were also somewhat separated from surrounding fluctuations, such that they appeared as discrete structures. These magnetic field enhancements were termed SLAMS (short large amplitude magnetic structures) (Schwartz and Burgess, 1991) and were proposed to be the 'building blocks' of the shock. Intrinsic to this picture were the concepts of a spatially extended and patchy shock transition, since the SLAMS collectively caused the thermalisation of the plasma, and temporal or cyclic evolution: new waves growing and steepened as they were convected back toward the shock, replacing those SLAMS which had passed downstream (Burgess, 1989; Schwartz and Burgess, 1991). These pulsations have formed the major focus for Cluster work related to the quasi-parallel shock.

At the time Cluster was launched there were many questions remaining unanswered about the nature of the quasi-parallel shock. Statistical studies of dual spacecraft observations suggested that SLAMS-like pulsations had a shorter correlation length than ULF waves: $\sim$1000 km (Greenstadt et al., 1982) compared with $\sim 0.5R_E$ (Le and Russell, 1990), but without multi-spacecraft observations it was not possible to determine their overall size or shape perpendicular to the plasma

flow direction, over what scale they were coherent, or whether they had internal structure. Their effect on the plasma was not well understood, and although the downstream region showed evidence for variations in the ion reflection properties of the shock (Thomsen et al., 1990), the relative contributions of a spatially extended and temporally varying shock were not well established. Information on SLAMS growth rates was limited by having only two point measurements with an intrinsic temporal/spatial variation ambiguity, and it was not known on what timescales they developed as they approached the shock surface. Simulation results suggested that they had a rapid growth rate, of the order of seconds or less (Giacalone et al., 1994), and that they might be refracted in a direction parallel to the shock as they were convected anti-sunward (Dubouloz and Scholer, 1995). More recently, predictions were also made of the evolution of the shape of the SLAMS structure with time from a ULF wave, to a symmetric magnetic field enhancement and finally to a steepened, asymmetric shape (e.g., Tsubouchi and Lembège, 2004). Simulations also predicted that steepened SLAMS should reflect a portion of the incoming solar wind flow, since their leading edges behave locally as quasi-perpendicular shocks.

6.2 Structure

6.2.1 Overview

With Cluster observations on a range of scales, we can start to address some open questions by exploiting the simultaneous four point measurements of multiple important observables, including magnetic field, electric field and waves, supported by high quality observations of other variables including plasma parameters, ion distributions and energetic particle fluxes. In addition, computer advances have allowed more sophisticated simulations to be made of the parallel shock (e.g., Scholer et al., 2003; Tsubouchi and Lembège, 2004), providing new results for comparison with observations. One difficulty, however, in studying well-developed quasi-parallel shocks using Cluster is the relatively small number of examples which have been observed at each scale. The first season of dayside observations was adversely affected by limited orbital coverage, but even in later years the number of clear quasi-parallel shocks remains small. This might be explained in part by the Cluster orbit, which tends to cross the bow shock at high latitudes near noon and only crosses the bow shock near the equator when apogee is located far on the magnetopause flanks. Cluster consequently samples a much higher proportion of low Mach number shocks than if the spacecraft were in an equatorial orbit and crossed the shock nearer the nose of the magnetopause.

In order to give an overview of a shock crossing, Figure 6.1 shows a quasi-parallel shock observed by Cluster 1 on February 2 (day 33) 2001. Data from the magnetic field instrument (FGM) (Balogh et al., 2001) and the ion instrument (CIS) (Rème et al., 2001) are shown. At the beginning of the interval Cluster was in the

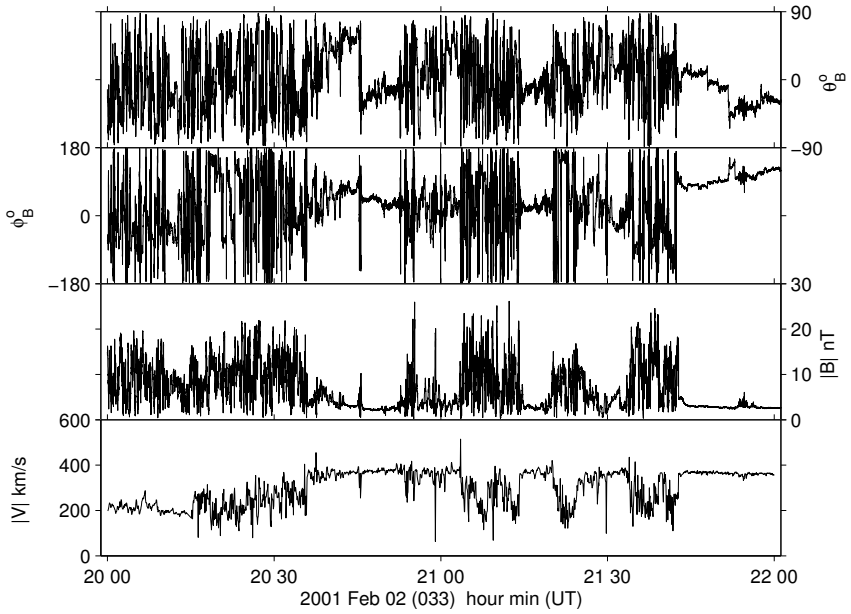

Figure 6.1. Magnetic field and velocity data recorded through a parallel shock crossing on February 2 2001. Data are from Cluster 1. Panels show magnetic field elevation (θ) and azimuthal (ϕ) angles in degrees, plotted in GSE co-ordinates, magnetic field magnitude $|\mathbf{B}|$ (nT), and plasma velocity $|\mathbf{V}|$ ($\mathrm{km\,s^{-1}}$). Cluster starts the interval in the magnetosheath, observes several shock crossings, and by the end of the interval is in the solar wind. Figure provided by E. A. Lucek.

magnetosheath. The spacecraft then made several crossings of the shock before entering the solar wind. The shock encounters are clearest in the plasma velocity, while the magnetic field data are very 'turbulent' and disturbed over an extended interval. It is worth noting that there are several intervals where the spacecraft returns to undisturbed solar wind, presumably in response to the shock moving due to changes in the upstream conditions.

The association of SLAMS and suprathermal ions is illustrated in Figure 6.2 which shows a close-up of a short interval within the extended transition covered by Figure 6.1. The top set of Figure 6.2 shows data from the CIS HIA sensor. The sub-panels show ion energy flux in counts per second from different directions indicated by the key on the right hand side. In this key, sunwards is toward the top of the page, earthward is toward the bottom of the page, with dusk and dawn toward the left and right respectively. HIA was operating in solar wind mode at this time, so the solar wind beam is measured separately and plotted in the top-most sub-panel. The bottom sub-panel here shows the flux integrated over a 4π solid angle. The bottom set of sub-panels of Figure 6.2 shows magnetic field and plasma velocity data in the same format as Figure 6.1. Just after 2045 UT Cluster

encountered an interplanetary discontinuity (which generated a hot flow anomaly, Eastwood et al. 2005, this issue) at which the interplanetary magnetic field turned to an orientation consistent with generating a quasi-parallel shock. The observed magnetic field then remained steady until about 2053 UT when suprathermal ions were seen in the duskward and sunward look directions, associated with enhancements in the magnetic field magnitude and depressions in the plasma flow velocity. Density enhancements can also be seen in the CIS spectra at the times of the magnetic field enhancements. At the very end of the interval Cluster briefly entered a region of shocked plasma.

6.2.2 Pulsations: Structure and scales

The first Cluster magnetic field observations of SLAMS when the tetrahedron scale was 600 km (Lucek et al., 2002) showed that, unexpectedly, significant variations in $|\mathbf{B}|$ occurred on these separations, despite the fact that the overall SLAMS extent exceeded the tetrahedron size as inferred from the overall duration and speed of the signatures.

This is illustrated in Figure 6.3 which shows the overall similarity between the observations at the different spacecraft, but at the same time the significant differences that can occur. In these examples the overall ordering of transitions indicate anti-sunward convection, but sometimes the ordering varies between leading and trailing edges and also between subsequent pulsations. The differences do not appear to be dominated by growth or decay in time: the SLAMS amplitudes are not ordered in time for example, but with only a few samples it is not possible to rule out that time evolution contributes to the observed signatures. Observations of ULF waves during the same pass showed that variations in $|\mathbf{B}|$ typically occur on shorter scales in SLAMS than in ULF waves, as expected from previous observations.

Observations of structures within a quasi-parallel shock when the Cluster spacing was 100 km were reported by Lucek et al. (2004), and shown in the bottom panels of Figure 6.4 which compares SLAMS on both scales. In this case the magnetic field strength enhancements on all spacecraft are better correlated, although with some small differences. Statistical analysis of the differences in $|\mathbf{B}|$ as a function of distance perpendicular to the flow suggests that while the SLAMS extent is much greater than 100 km, the gradient scale appears to be of the order of 100-150 km.

The attempts to use Cluster observations taken at different scales to infer the intrinsic scale of SLAMS has indicated an unexpected paradox. In order use Cluster timings to obtain velocities and orientations (as in the case of the quasi-perpendicular shock), it is necessary that all four spacecraft measure similar profiles. However, determining scale lengths transverse to either flow or motion of structures requires differences between the measured profiles. So on the one hand the requirement is closely positioned observation points, but on the other well separated ones. This suggests that a better separation strategy with unequal separations might have been

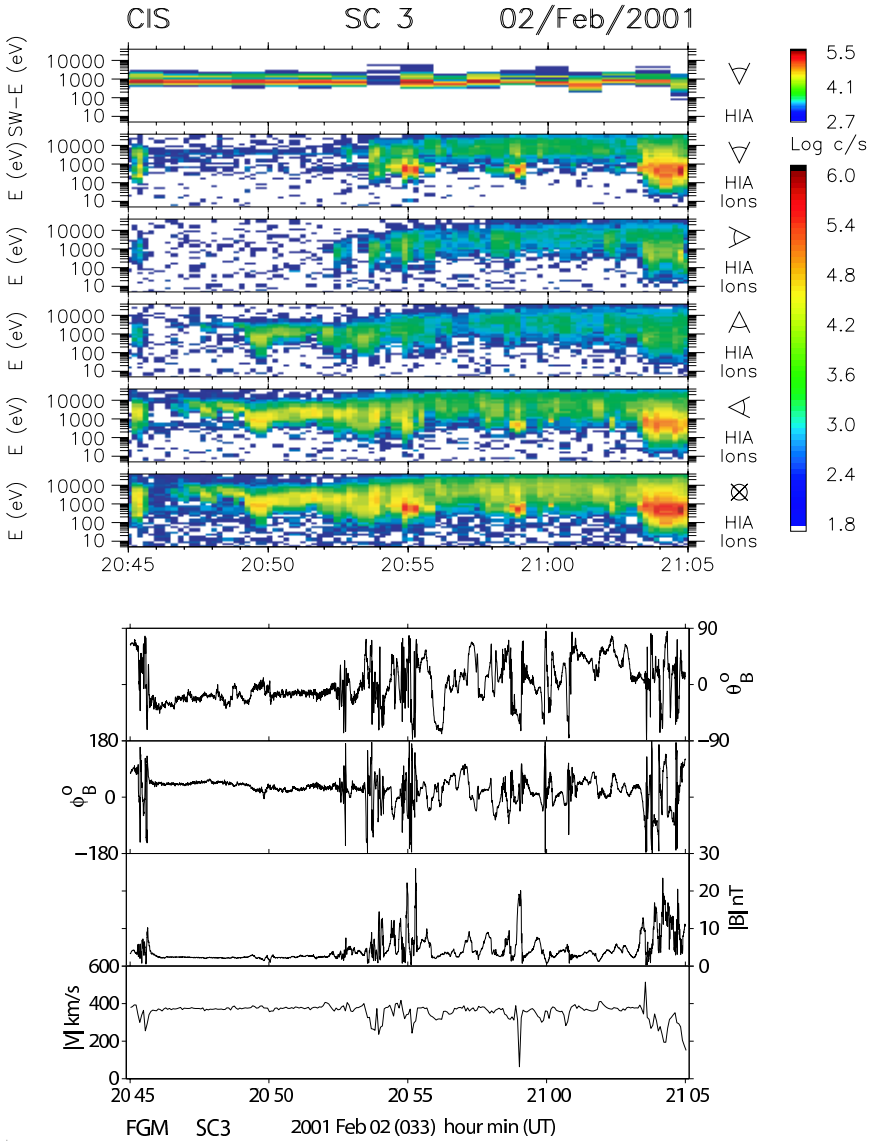

Figure 6.2. Extended transition from clean solar wind (left) to the magnetosheath (far right) showing the appearance and evolution of diffuse ions (top) together with magnetic fluctuations at the bow shock under quasi-parallel conditions. The top panel shows data from the CIS HIA instrument. Subpanels show ion energy flux in counts per second from different directions indicated by the key on the right hand side: sunwards (up); dusk (left); dawn (right); earthward (down). HIA was operating in solar wind mode at this time, so the solar wind beam is measured separately and plotted in the top sub-panel. The bottom sub-panel shows the flux integrated over a 4π solid angle. The bottom panel shows magnetic field and plasma velocity data in the same format as Figure 6.1. Figure provided by E. A. Lucek, CIS data courtesy of the CIS team.

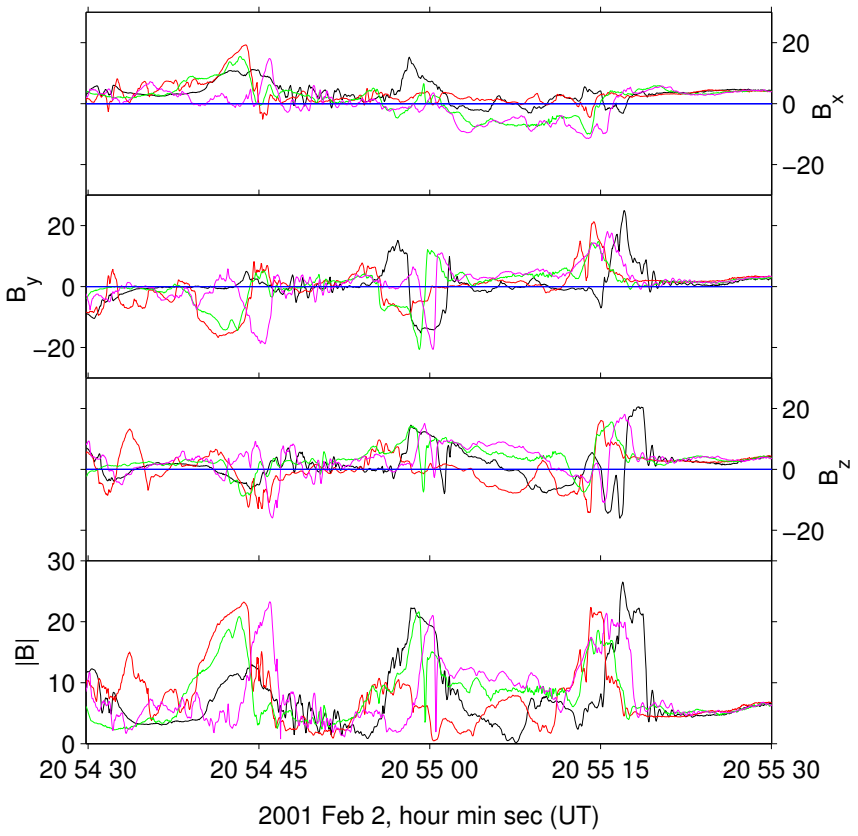

Figure 6.3. Magnetic field data (components in GSE and magnitude) from the four Cluster spacecraft at 22 vectors/s showing magnetic field enhancements within a pulsation region. The spacecraft separations are in the range 400–800 km. From Lucek et al. (2002).

possible for the quasi-parallel shock, although with some loss of information on the orientation of structures.

This paradox is evident in the studies of SLAMS at spacecraft separations of 600 km and 100 km. When the Cluster tetrahedron scale was ∼600 km, there were relatively few SLAMS where the spacecraft profiles were similar enough to calculate the SLAMS orientation; while at a separation of ∼100 km, the method can be used more comprehensively, but there is not any information available over scales larger than the spacecraft separation. A possible future study would be to test statistically whether (single spacecraft) minimum variance analysis is a good measure of the SLAMS orientation locally using timings data for small spacecraft separations. Consequently, SLAMS observations at large tetrahedron scales could be explored for signatures of curvature or acceleration.

6.2.3 Pulsations: Fields and particles

The Cluster EFW experiment measures the spacecraft potential at relatively high cadence (5 samples/second), which serves as a proxy for the electron density. Behlke et al. (2003) presented the first high resolution electric field and spacecraft potential measurements at SLAMS. It was found that the density and magnetic field strength were correlated, confirming the earlier indications that SLAMS were fast mode structures. Timing analysis was used to derive the SLAMS velocity in the spacecraft frame. This differed from the background solar wind velocity and the SLAMS pulsation was found to be propagating sunward in the plasma frame. However, the motional electric field computed using the SLAMS velocity matched the measured electric field within the SLAMS, while a systematic discrepancy was found if the motional electric field was calculated using the background solar wind velocity. Behlke et al. (2003) inferred therefore that, locally, the plasma within the SLAMS moved at the same speed as the SLAMS perturbation, although the SLAMS moved relative to the background solar wind. The authors also noted that in some cases there was a plasma density depletion behind the SLAMS (in the SLAMS frame), indicating some kind of wake structure, and that the presence of differences between the four spacecraft suggested that this wake varied on scales of ~ 600 km.

Examination of high resolution measurements of the electric field within SLAMS showed that on short time scales local discrepancies were observed between the measured and calculated electric fields. Behlke et al. (2003) noted that similar small scale electric field spikes have been observed in simulations of SLAMS (Lembège et al., 2004). These studies of high resolution electric fields at SLAMS were extended by Behlke et al. (2004) who presented evidence of solitary waves within them. The observed waves occurred as bipolar (sometimes tripolar) pulses with a parallel scale of the order of 10 Debye lengths, and peak-to-peak amplitudes of up to 65 mV m^{-1}. The velocities of these very small structures were derived using the four probes on a single spacecraft as an interferometer. Solitary waves observed in the auroral acceleration region and at other magnetospheric boundaries have been studied extensively. However the examples observed in the shock pulsations, with a propagation velocity of 400 - 1200 km s^{-1}, being higher than the typical ion thermal speed, have properties which make them difficult to explain using any of the current theories of solitary waves. Although they present an interesting problem in terms of plasma physics, these solitary wave structures have no obvious associated net potential drop. Therefore, although they might play a role in electron thermalisation, the authors noted that there was insufficient evidence to conclude that they are important for the structure of SLAMS.

The relationship between magnetic field strength and electron density (as indicated by the spacecraft potential) has been investigated by Stasiewicz et al. (2003). They suggest that some SLAMS have no associated plasma density variations, but that for those with a positive density enhancement, corresponding to a fast mode

structure, the density and field changes are not exactly in phase. The maximum in the field magnitude occurs during the density increase. Stasiewicz et al. (2003) present a descriptive model, based on simple momentum conservation and a polytropic equation of state, that is used to explain the profiles in density and field. The explanation is based on assuming compression and then heating in stages through the SLAMS. Although possibly appropriate to some of the observed structures, it is clear from, for example, other work reported here that if there is such variability in pulsation signatures then only a rigorous statistical study will be convincing.

Two examples of SLAMS are shown in Figure 6.4 showing the magnetic field magnitude and the negative spacecraft potential ($-V_{SC}$) which can be used as a proxy for the plasma density (Gustafsson et al., 2001). The top panel shows data for a Cluster separation scale of $\sim$600 km, whilst the bottom panel has data for a separation scale of $\sim$100 km. The correlation between data from different spacecraft as a function of separation scale has already been discussed. Here we note that the correlation between field magnitude and density is not always the same, even within a single event. This is most clearly seen in the top panel where the magnitude of the SLAMS in $|\mathbf{B}|$ is smaller at Cluster 1 than at Cluster 3 or 4, whilst the magnitude of $-V_{SC}$ is approximately the same at these three spacecraft. It can also be noted that the times at which $|\mathbf{B}|$ and $-V_{SC}$ increase differ within a particular SLAMS event. This points to the importance of nonlinear, time non-stationary processes in the SLAMS growth and evolution.

A key issue in understanding the relationship between pulsations and the overall shock transition is their role in the development of ion thermalisation. Before Cluster crossed the SLAMS magnetic field enhancement shown in the lower panel of Figure 6.4, the spacecraft observed a region of enhanced wave activity in the magnetic field, where the correlation between the signals at the different spacecraft was lower; this corresponds to the wake region behind the SLAMS. The implication is that variations occurred on smaller spatial scales in this region: on the scale of the order of the ion inertial length or even less. This might be related to the partial plasma thermalisation, visible in both the velocity moment and CIS ion distributions shown in Figure 6.5. In comparison with the ion distribution in undisturbed solar wind plasma, the plasma on the left-hand side of the SLAMS (downstream in the SLAMS frame) is hotter, slower and deflected slightly. The middle of the three distributions shows a slightly heated solar wind beam, and an additional population of sunward moving ions, consistent with reflection from the SLAMS. Further work is required to relate such observations to the orientation of the pulsations, and also to identify any instability responsible for the thermalization in the wake region.

6.3 Diffuse Ion Acceleration

Since the early observations of ions upstream of Earth's quasi-parallel bow shock by Asbridge et al. (1968) and by Lin et al. (1974) upstream ions with energies just above the solar wind energy up to several hundred keV have been under investiga-

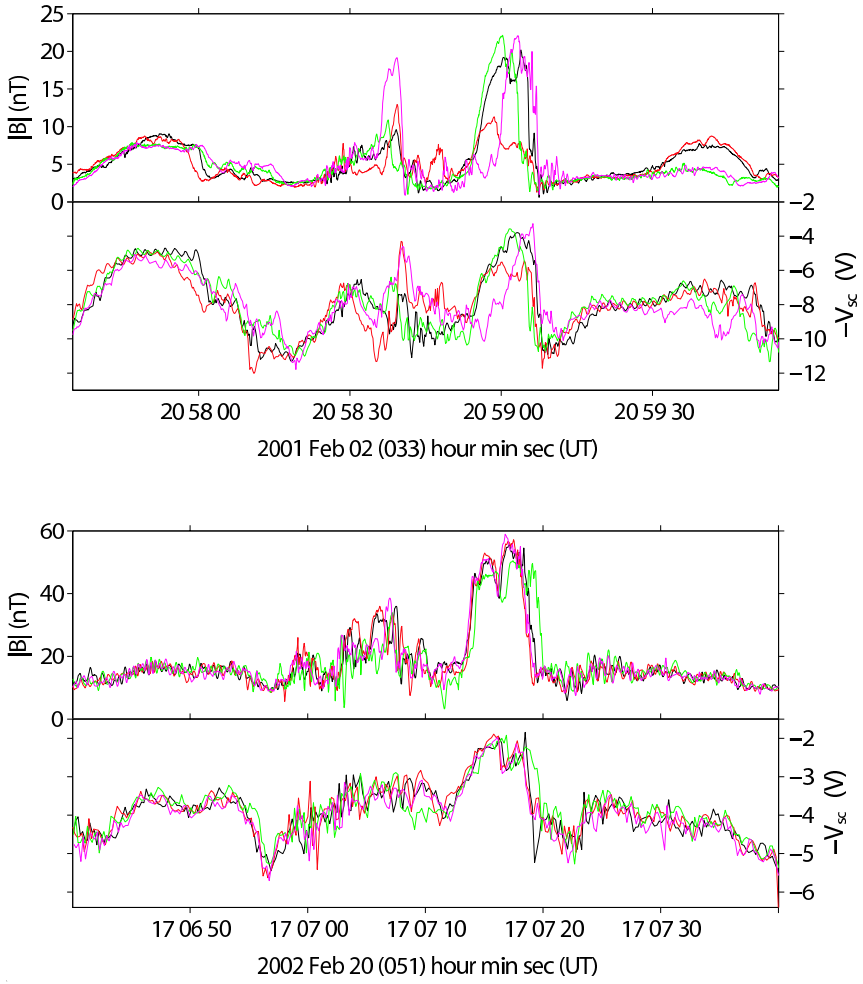

Figure 6.4. Two examples of SLAMS observed in magnetic field magnitude $|\mathbf{B}|$, (top sub-panel) and negative spacecraft potential $-V_{sc}$, (bottom sub-panel). The case in the top panel was observed when the tetrahedron scale was ∼600 km, and the lower panel shows an example when the tetrahedron scale was reduced to ∼100 km. Figure provided by E. A. Lucek, EFW spacecraft potential data courtesy of R. Behlke.

tion (see also Section 2.3 of Bale et al., 2005). A number of studies have established two different sources for these ions: the so-called magnetospheric bursts at energies above a few hundred keV and the bow-shock associated, so-called diffuse particles. Diffuse ion events last up to several hours and extend in energy up to ∼ 150 keV (Ipavich et al., 1981; Scholer et al., 1981). The spectra of protons and alpha particles in these events are generally well described as exponentials in energy per

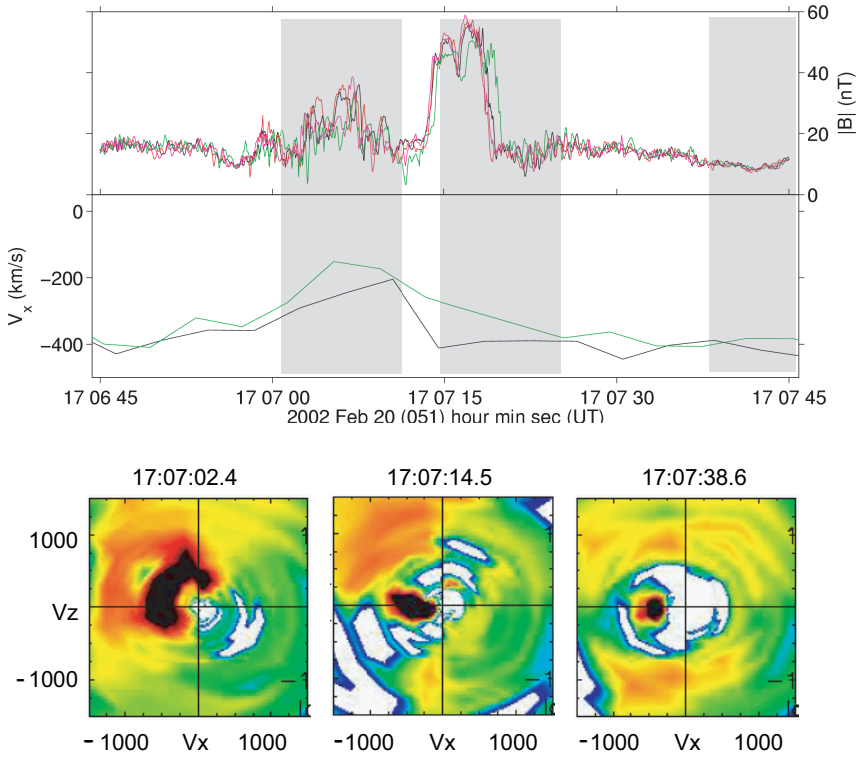

Figure 6.5. Ion reflection associated with SLAMS. The top two panels show magnetic field magnitude and plasma velocity in the X_{GSE} direction. The three shaded areas show the approximate times over which the three ion distributions shown below were accumulated. Each ion distribution shows ion flux plotted on a colour scale where blue and green indicate low fluxes, and black indicates high flux. Each distribution is a cut through $V_Y\,(GSE) = 0$ and shows V_X on the ordinate and V_Z on the abscissa. Figure provided by E. A. Lucek, CIS data courtesy of I. Dandouras.

charge, and the ratio of the fluxes of the two species is constant as a function of energy per charge (Ipavich et al., 1981). The distribution of diffuse ions is rather isotropic with a shock directed bulk velocity slower than the solar wind speed. Hoppe et al. (1981) demonstrated that there is a one-to-one correlation between the presence of diffuse upstream ions and the occurrence of hydromagnetic waves in the foreshock region. This has led to the widely adopted picture of an intensive interplay between the waves and energetic ions: the waves are thought to constitute scattering centres for the ions, which results in a diffusive transport. If transport is diffusive these particles will experience the shock compression, which leads to first order Fermi acceleration (e.g., Axford et al., 1977, see also reviews by Scholer, 1985 and Forman and Webb, 1985). The diffusive shock acceleration mechanism has often been challenged by the proposition that all upstream ion enhancements at

all major magnetospheres, in particular that of Earth's, are exclusively of magnetospheric origin (Sarris et al., 1987). A prerequisite for a first order Fermi mechanism to occur at Earth's bow shock is that the particles do not stream scatter free, as implied by the magnetospheric escape model in which ions from the magnetopause propagate through the magnetosheath upstream against the convecting solar wind.

Steady state diffusive theory at a planar shock predicts that the density of energetic ions (energy E) falls off exponentially from the shock front into the upstream region, with an e-folding distance given by $L(E) = \kappa(E)/v_{sw}$, where $\kappa(E)$ is the spatial diffusion coefficient parallel to the mean field for particles of energy E, and v_{sw} is the solar wind speed (here it is assumed that the shock normal, the magnetic field and the solar wind velocity are aligned). In order to demonstrate that the upstream ions are indeed subject to diffusive transport it is thus of great interest to determine the spatial gradient along the magnetic field. Previous determinations of the spatial variation of upstream particle intensity used single spacecraft data and had therefore to be done on a statistical basis. Ipavich et al. (1981) have shown by analysing 33 upstream particle events that at ~ 33 keV the differential proton flux decreased exponentially with an e-folding distance of $R = 7 \pm 2\mathrm{R_e}$ upstream of the shock. Trattner et al. (1994) performed a statistical study of about 300 upstream events. They determined the distance to the shock along the interplanetary magnetic field and corrected the shock position according to the actual solar wind ram pressure. From a linear regression they determined an e-folding distance of $R = 4.8 \pm 0.1\mathrm{R_e}$ at 20 keV. The e-folding distance increases with energy and varies from $3.2 \pm 0.2\mathrm{R_e}$ at 10 keV to $9.3 \pm 1\mathrm{R_e}$ at ~ 67 keV.

Although these statistical results seem to prove the importance of diffusive transport in the upstream region they are hampered by the possibility that the intensity in the upstream region at one location may vary widely from event to event according to interplanetary conditions. The small correlation coefficient of 0.65 of the linear regression analysis of Trattner et al. (1994) may even be taken as evidence that the intensity is more or less constant along the field and that the spread is due to sampling of events with varying intensity. Cluster provides the unique opportunity to investigate the spatial gradient of upstream diffuse ions during times of large spacecraft separation distance. Recent analysis of Cluster data by Kis et al. (2004) provides direct evidence that the upstream particles undergo a diffusive transport.

Kis et al. (2004) have investigated a 10 hour time period on 18 February 2003 when Cluster was upstream of the quasi-parallel bow shock on an inbound orbit. Figure 6.6 shows from top to bottom the solar wind v_x velocity, the three components of the interplanetary magnetic field as measured by FGM on Cluster 1, and the partial density of upstream ions in the energy range 24 - 32 keV as measured by the CIS-HIA instrument at two spacecraft, at Cluster 1 (black line) and at Cluster 3 (green line). Also shown by inserts are projections of the spacecraft orbits and the bow shock onto the GSE $x-y$ and $x-z$ planes. During this time period Cluster 1 is about $1.5\,\mathrm{R_e}$ closer to the bow shock than Cluster 3. As can be seen from Fig-

ure 6.6, Cluster 1 exhibits a higher partial density during the entire time interval than Cluster 3: the partial density ratio between the two spacecraft varied from a few percent up to 50%. The Cluster spacecraft were magnetically connected to the quasi-parallel bow shock throughout. From the 8 spin (32 sec) averaged magnetic field data, the distance of the spacecraft along the magnetic field to the bow shock intersection point has been determined. For determination of the bow shock position, the Peredo et al. (1995) model has been employed and was expanded to the actual bow shock location by using the spatial position of the bow shock during the first inbound shock crossing of SC1. From this model an average local magnetic field-shock normal angle at the magnetic field-bow shock intersection point of $20^\circ \pm 8^\circ$ has been determined for the whole 10 hour time period. The ratio between the difference of the partial densities at the two spacecraft and the difference between the spacecraft distances along the magnetic field to the bow shock intersection point then gives gradient values at various distances. Figure 6.7 shows these partial density gradients for the 24 - 32 keV energy range in $\mathrm{cm}^{-3}\mathrm{R_e}^{-1}$ versus distance from the bow shock along the magnetic field averaged in seven $1\mathrm{R_e}$ wide distance bins. Since the data points in this logarithmic versus linear representation can be fit by a straight line the gradient is very well represented by an exponential as a function of distance from the shock.

The procedure described above has been performed for the 4 highest energy channels of the CIS-HIA instrument. The resulting *e*-folding distances L for the partial densities in each of the 4 energy channels are shown in Figure 6.8. The error bars indicate the 1σ uncertainties due to the fitting procedure. As can be seen from Figure 6.8 the *e*-folding distance $L(E)$ of the partial density gradients depends approximately linearly on energy E and increases from $\sim 0.5\,\mathrm{R_e}$ at $\sim$11 keV to $\sim 2.8\,\mathrm{R_e}$ at $\sim$27 keV.

In the simple steady state model of Fermi acceleration at a planar shock, the *e*-folding distance is given by $L(E) = \kappa(E)/v_{sw}$. Since $\kappa(E) = d(E)v/3$, where $d(E)$ is the diffusion length and v is the particle velocity (in the plasma frame) we can write $d(E) = 3L(E)(E_{sw}/E)^{1/2}$, where E is the particle energy and E_{sw} is the bulk energy of the solar wind. Thus the diffusion length has an energy dependence of $d(E) \propto E^{0.5}$. From the measured *e*-folding distance and from the solar wind speed Kis et al. (2004) obtained at 30 keV a mean free path of $2.4\,\mathrm{R_e}$. The important result here is that these energetic particles are clearly undergoing a diffuse transport process in the upstream region. It is thus unavoidable that they feel the shock compression and are necessarily accelerated by a first order Fermi acceleration process at the shock. The analysis by Kis et al. (2004) can only be considered as a first step in trying to gain insight into the injection and acceleration process at the quasi-parallel bow shock. For instance it is not clear whether the small *e*-folding distances found during this event are due to the extremely large solar wind velocity ($\sim 640\,\mathrm{km\,s^{-1}}$). Thus other events with considerably smaller solar wind speed have to be analysed. The strong scattering is due to the waves produced by

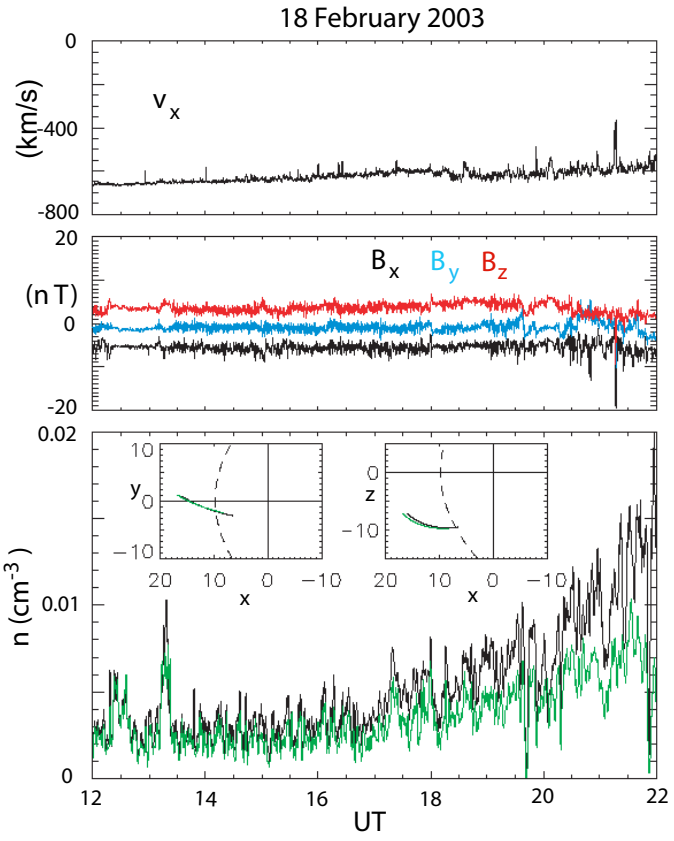

Figure 6.6. Data from which the spatial gradient in diffuse ions, and hence the scattering mean free path, have been determined. From top to bottom: Solar wind velocity component v_x and magnetic field components B_x (black line), B_y (blue line), B_z (red line) as measured on Cluster 1, partial ion density in the 24 - 32 keV energy range as measured at Cluster 1 (black line) and Cluster 3 (green line). Also shown in the lower panel are projections of the spacecraft orbits and bow shock onto the $x-y$ and $x-z$ plane, respectively. From Kis et al. (2004).

the particles themselves. Quasi-linear theory predicts an energy dependence of the diffusion coefficient depending on the slope of the magnetic field power spectrum. Comparison of the spectral exponent of the magnetic field fluctuations with the energy dependence of the diffusion coefficient and of the absolute value of the power in the fluctuations with the magnitude of the diffusion coefficient would provide a test of quasi-linear pitch-angle theory, which is widely applied to other astrophysical settings. The combined data set of magnetic field fluctuations and particle data should provide new insight into injection and acceleration at the quasi-linear bow shock.

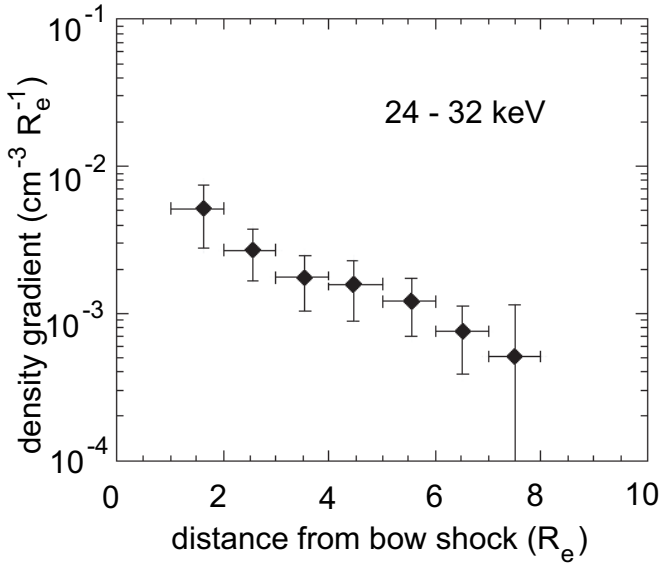

Figure 6.7. Average partial ion density gradient in the 24-32 keV energy range versus distance from the bow shock. From Kis et al. (2004).

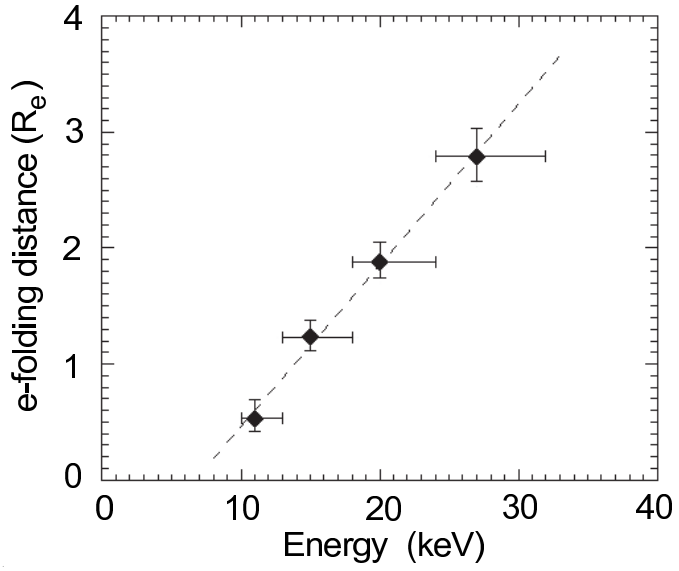

Figure 6.8. The e-folding distance obtained by fitting an exponential to the partial density gradient in 4 energy channels. From Kis et al. (2004).

6.4 Summary

The quasi-parallel regions of the Earth's bow shock, where the interplanetary magnetic field is nearly parallel to the nominal shock normal, provide a complex environment in which multi-streaming collisionless plasma and field components thrive and interact both to effect an overall shock transition, decelerating and heating the incident solar wind, and to accelerate a sub-population of particles to higher energies through the universally invoked Fermi process. The intrinsically unsteady and turbulent nature of this region has made it somewhat less amenable to single spacecraft studies (by comparison to the quasi-perpendicular bow shock reported in Section 2.1 of Bale et al., 2005, this issue), while also shifting the emphasis somewhat from the pure shock transition in terms of dissipation and heating to a more heterogeneous perspective.

Key Cluster results to date as reported in this Chapter include:

1. The revelation that Short Large Amplitude Structures (SLAMS), which prevail under quasi-parallel shock conditions, have considerable sub-structure on scales < 600 km despite their apparent monolithic appearance on scales ~ 6000 km.
2. New results on the electric fields within SLAMS, confirming in some sense their monolithic macroscopic role.
3. Quantitative analysis of the diffusive scattering length in the upstream 'foreshock' region, confirming the operation of a Fermi-like process there.

These results represent only a fraction of the potential of the Cluster dataset, particularly since the later stages of the mission will see the spacecraft separations increase to scales commensurate with the foreshock scales of 10,000's of km.

Acknowledgements

The contributions of HK and EM were partially supported under NASA Grants NAG5-10131 and NAG5-11804. PPARC (UK) support for this work includes fellowships (TSH and EL) and research grants (DB, SJS, SNW).

References

Asbridge, J. R., S. J. Bame, and I. B. Strong: 1968, 'Outward flow of protons from the Earth's bow shock'. *J. Geophys. Res.* **73**(12), 5777.

Axford, W. I., E. Leer, , and G. Skadron: 1977, 'The acceleration of cosmic rays by shock waves'. In: *Proc. Int. Conf. Cosmic Rays 15th*. p. 132.

Bale, S. D., M. A. Balikhin, T. S. Horbury, V. V. Krasnoselskikh, H. Kucharek, E. Möbius, S. N. Walker, A. Balogh, D. Burgess, B. Lembège, E. A. Lucek, M. Scholer, S. J. Schwartz, and M. F. Thomsen: 2005, 'Quasi-perpendicular shock structure and processes'. *Space Sci. Rev.* **this issue**.

Balogh, A., C. M. Carr, M. H. Acuña, M. W. Dunlop, T. J. Beek, P. Brown, K. H. Fornacon, E. Georgescu, K. H. Glassmeier, J. Harris, G. Musmann, T. Oddy, and K. Schwingenschuh: 2001,

'The Cluster magnetic field investigation: Overview of in-flight performance and initial results'. *Ann. Geophys.* **19**, 1207–1217.

Behlke, R., M. André, S. D. Bale, J. S. Pickett, C. A. Cattell, E. A. Lucek, and A. Balogh: 2004, 'Solitary structures associated with short large-amplitude magnetic structures (SLAMS) upstream of the Earth's quasi-parallel bow shock'. *Geophys. Res. Lett.* **31**, L16805, doi:10.1029/2004GL019524.

Behlke, R., M. André, S. C. Buchert, A. Vaivads, A. I. Eriksson, E. A. Lucek, and A. Balogh: 2003, 'Multi-point electric field measurements of Short Large-Amplitude Magnetic Structures (SLAMS) at the Earth's quasi-parallel bow shock'. *Geophys. Res. Lett.* **30**, 1177, doi:10.1029/2002GL015871.

Burgess, D.: 1989, ' Cyclic behaviour at quasi-parallel collisionless shocks'. *Geophys. Res. Lett.* **16**, 345–348.

Dubouloz, N. and M. Scholer: 1995, 'Two-dimensional simulations of magnetic pulsations upstream of the Earth's bow shock'. *J. Geophys. Res.* **100**, 9461–9474.

Eastwood, J., E. A. Lucek, C. Mazelle, K. Meziane, Y. Narita, J. Pickett, and R. Treumann: 2005, 'The Foreshock'. *Space Sci. Rev.* **this issue**.

Forman, M. A. and G. M. Webb: 1985, 'Acceleration of energetic particles'. *Washington DC American Geophysical Union Geophysical Monograph Series* **35**, 91–114.

Giacalone, J., S. J. Schwartz, and D. Burgess: 1993, ' Observations of suprathermal ions in association with SLAMS '. *Geophys. Res. Lett.* **20**, 149–152.

Giacalone, J., S. J. Schwartz, and D. Burgess: 1994, 'Artificial spacecraft in hybrid simulations of the quasi-parallel Earth's bow shock: Analysis of time series versus spatial profiles and a separation strategy for Cluster'. *Ann. Geophys.* **12**, 591–601.

Gosling, J. T., M. F. Thomsen, S. J. Bame, W. C. Feldman, G. Paschmann, and N. Sckopke: 1982, 'Evidence for specularly reflected ion upstream from the quasi-parallel bow shock'. *Geophys. Res. Lett.* **9**, 1333–1336.

Greenstadt, E. W., M. M. Hoppe, and C. T. Russell: 1982, 'Large-amplitude magnetic variations in quasi-parallel shocks: correlation lengths measured by ISEE 1 and 2'. *Geophys. Res. Lett.* **9**, 781–784.

Gustafsson, G., M. André, T. Carozzi, A. Eriksson, C.-G. Fälthammar, R. Grard, G. Homgren, J. Holtet, N. Ivchenko, T. Karlsson, Y. Khotvaintsev, S. Klimov, H. Laakso, G. Marklund, F. Mozer, K. Mursula, A. Pedersen, B. Popielawska, S. Savin, K. Stasiewicz, P. Tanskanen, A. Vaivads, and J.-E. Wahlund: 2001, 'First results of electric field and density observations by Cluster EFW based on initial months of operation'. *Ann. Geophys.* **19**, 1219–1240.

Hoppe, M. M., C. T. Russell, L. A. Frank, T. E. Eastman, and E. W. Greenstadt: 1981, 'Upstream hydromagnetic waves and their association with backstreaming ion populations - ISEE 1 and 2 observations'. *J. Geophys. Res.* **86**, 4471–4492.

Ipavich, F. M., A. Galvin, G. Gloeckler, M. Scholer, and D. Hovestadt: 1981, 'A statistical survey of ions observed upstream of the earth's bow shock - Energy spectra, composition, and spatial variation'. *J. Geophys. Res.* **86**, 4337–4342.

Kis, A., M. Scholer, B. Klecker, E. Möbius, E. Lucek, H. Réme, J. M. Bosqued, L. M. Kistler, and H. Kucharek: 2004, 'Multispacecraft observations of diffuse ions upstream of Earth's bow shock'. *Geophys. Res. Lett.* **31**, L20801, doi:10.1029/2004GL020759.

Le, G. and C. T. Russell: 1990, ' A study of the coherence length of ULF waves in the Earth's foreshock '. *J. Geophys. Res.* **95**, 10703–10706.

Le, G. and C. T. Russell: 1992, 'A study of ULF wave foreshock morphology ? II: Spatial variation of ULF waves'. *Planet. Space Sci.* **40**, 1215–1225.

Lembège, B., J. Giacalone, M. Scholer, T. Hada, M. Hoshino, V. Krasnoselskikh, H. Kucharek, P. Savoini, and T. Terasawa: 2004, 'Selected problems in collisionless-shock physics'. *Space Science Reviews* **110**, 161–226.

Lin, R. P., C. I. Meng, and K. A. Anderson: 1974, '30 -100 keV protons upstream from the Earth bow shock'. *J. Geophys. Res.* **79**, 489.

Lucek, E. A., T. S. Horbury, A. Balogh, I. Dandouras, and H. Rème: 2004, 'Cluster observations of structure at quasi-parallel bow shocks'. *Ann. Geophys.* in press.

Lucek, E. A., T. S. Horbury, M. W. Dunlop, P. J. Cargill, S. J. Schwartz, A. Balogh, P. Brown, C. Carr, K. H. Fornacon, and E. Georgescu: 2002, 'Cluster magnetic field observations at a quasi-parallel bow shock'. *Ann. Geophys.* **20**, 1699–1710.

Peredo, M., J. A. Slavin, E. Mazur, and S. A. Curtis: 1995, 'Three-dimensional position and shape of the bow shock and their variation with Alfvenic, sonic and magnetosonic Mach numbers and interplanetary magnetic field orientation'. *J. Geophys. Res.* **100**(9), 7907–7916.

Rème, H., C. Aoustin, J.-M. Bosqued, and et al.: 2001, 'First multispacecraft ion measurements in and near the Earth's magnetosphere with the identical Cluster ion spectrometry (CIS) experiment'. *Ann. Geophys.* **19**, 1303–1354.

Sarris, E. T., G. C. Anagnostopoulos, and S. M. Krimigis: 1987, 'Simultaneous measurements of energetic ion (50 keV and above) and electron (220 keV and above) activity upstream of Earth's bow shock and inside the plasma sheet - Magnetospheric source for the November 3 and December 3, 1977 upstream events'. *J. Geophys. Res.* **92**(11), 12083–12096.

Scholer, M.: 1985, 'Diffusive acceleration'. *Washington DC American Geophysical Union Geophysical Monograph Series* **35**, 287–301.

Scholer, M., F. M. Ipavich, and G. Gloeckler: 1981, 'Beams of protons and alpha particles greater than approximately 30 keV/charge from the Earth's bow shock'. *J. Geophys. Res.* **86**, 4374–4378.

Scholer, M., H. Kucharek, and I. Shinohara: 2003, 'Short large-amplitude magnetic structures and whistler wave precursors in a full-particle quasi-parallel shock simulation'. *J. Geophys. Res.* **108**, 1273, doi:10.1029/2002JA009820.

Schwartz, S. J. and D. Burgess: 1991, ' Quasi-parallel shocks: A patchwork of three-dimensional structures'. *Geophys. Res. Lett.* **18**, 373–376.

Stasiewicz, K., M. Longmore, S. Buchert, P. K. Shukla, B. Lavraud, and J. Pickett: 2003, 'Properties of fast magnetosonic shocklets at the bow shock'. *Geophys. Res. Lett.* **30**, 2241, doi:10.1029/2003GL017971.

Thomsen, M. F., J. T. Gosling, S. J. Bame, and T. G. Onsager: 1990, 'Two-state heating at quasi-parallel shocks'. *J. Geophys. Res.* **95**, 6363–6374.

Thomsen, M. F., J. T. Gosling, and C. T. Russell: 1988, ' ISEE studies of the quasi-parallel bow shock'. *Adv. Space. Res.* **8**, 9175–9178.

Trattner, K. J., E. Mobius, M. Scholer, B. Klecker, M. Hilchenbach, and H. Luehr: 1994, 'Statistical analysis of diffuse ion events upstream of the Earth's bow shock'. *J. Geophys. Res.* **99**(18), 13389.

Tsubouchi, K. and B. Lembège: 2004, 'Full particle simulations of short large-amplitude magnetic structures (SLAMS) in quasi-parallel shocks'. *J. Geophys. Res.* **109**, A02114, doi: 10.1029/2003JA010014.